

Vasoactive Intestinal Peptide Receptor Scintigraphy

Irene Virgolini, Amir Kurtaran, Markus Raderer, Maria Leimer, Peter Angelberger, Ernst Havlik, Shuren Li, Werner Scheithauer, Bruno Niederle, Peter Valent and Hans-Georg Eichler

Departments of Nuclear Medicine, Clinical Pharmacology, Internal Medicine I, Division of Oncology and Division of Hematology, Biomedical Engineering and Physics, General Surgery and The Ludwig Boltzmann Institute for Nuclear Medicine, University of Vienna, Vienna, Austria and Department of Radiochemistry, Research Center Seibersdorf, Austria

This study presents the biodistribution, safety and absorbed dose of ^{123}I -VIP administered to 18 patients with intestinal adenocarcinomas or endocrine tumors. **Methods:** To achieve high-specific activity, ^{123}I -VIP was purified by HPLC. Following intravenous administration of ^{123}I -VIP (172 ± 17 MBq (4.65 ± 0.5 mCi); <300 pmole (<1 μg)/patient), sequential images were recorded during the initial 30 min. Thereafter, whole-body images were acquired in anterior and posterior views at various time points. Dosimetry calculations were performed on the basis of gamma camera data, urine, feces and blood activities. **Results:** After injection of labeled peptide, the lung was the primary site of ^{123}I -VIP uptake. Peak lung activity represented $40\% \pm 7\%$ of the injected dose at 0.7 hr and declined to $21\% \pm 7\%$ at 3.5, to $14\% \pm 3\%$ at 7 and to $8\% \pm 4\%$ 22 hr postinjection. Radioactivity was excreted into the urine and amounted to $37\% \pm 16\%$ of the injected dose within 4, $68\% \pm 12\%$ within 8, $82\% \pm 16\%$ within 16 and $93\% \pm 8\%$ within 24 hr postinjection. The mean effective half-life of ^{123}I -VIP in the lungs was 2.2 and 6 hr in the urinary bladder. The highest radiation absorbed doses were calculated for the lungs [67 $\mu\text{Gy}/\text{MBq}$ (248 mrad/mCi)], urinary bladder [77 $\mu\text{Gy}/\text{MBq}$ (284 mrad/mCi)] and thyroid gland [104 $\mu\text{Gy}/\text{MBq}$ (386 mrad/mCi)]. The effective dose was 28 $\mu\text{Sv}/\text{MBq}$ (104 mrem/mCi). **Conclusion:** HPLC-purified ^{123}I -VIP shows favorable dosimetry and is a safe and promising peptide tracer for localization of tumors expressing receptors for VIP.

Key Words: vasoactive intestinal peptide; receptor imaging; adenocarcinomas; endocrine tumors

J Nucl Med 1995; 36:1732-1739

In the last few years, increasing efforts have been undertaken to introduce peptide receptor-specific radioligands, including somatostatin analogs (1) and VIP (2) for the in vivo application in humans. VIP is a 28-amino acid peptide of the glucagon-secretin family first characterized

from porcine duodenum by Said and Mutt (3). The peptide has a molecular weight of 3326 Daltons and maintains a broad range of biologic activities. Originally, VIP was characterized as a vasodilatory substance with potent effects on peripheral and pulmonary blood pressures (3). VIP also stimulates the secretion of various hormones (4-6) and is responsible for the Verner Morrison syndrome in patients with VIP-secreting tumors (7,8). Furthermore, VIP is an important immunomodulator (9,10) and promotes growth and proliferation of normal and malignant cells (11-14). The actions of VIP are mediated by cell surface membrane receptors. VIP receptors are widely distributed throughout the body, including peripheral blood cells (10,11,15), the gastrointestinal tract (15,16), lungs (17) and kidneys (18).

Recently, we were able to demonstrate that various tumor cells express significantly higher amounts of VIP receptors as compared with normal peripheral blood cells or tissues (11). The high expression of VIP receptors provided the basis for the clinical use of radiolabeled VIP for the in vivo localization of intestinal adenocarcinomas and endocrine tumors (2). In a previous study of 79 patients (2), high ^{123}I -VIP scan sensitivity was found for primary or recurrent colorectal, pancreatic and gastric adenocarcinomas as well as for the visualization of liver and lymph node metastases. Because most tumors co-express VIP and somatostatin receptors (11), VIP receptor scans were also compared with somatostatin/octreotide receptor scans in 38 patients (2). A significant advantage of VIP receptor imaging over octreotide receptor imaging was demonstrable in patients with adenocarcinomas, whereas the scanning results of both peptide receptor scans were almost identical in patients with intestinal endocrine tumors (2). We now present our data on the radiochemical preparation of ^{123}I -VIP, its functional capacity, whole-body biodistribution and radiation absorbed dose estimates in humans.

METHODS

Radiopharmaceutical Preparation, Purity and Biological Activity of Iodine-123-VIP

VIP (H-His-Ser-Asp-Ala-Val-Phe-Thr-Asp-Asn-Tyr-Thr-Arg-Leu-Arg-Lys-Gln-Met-Ala-Val-Lys-Lys-Tyr-Leu-Asn-Ser-Ile-Leu-Asn-NH₂) was synthesized by peptide synthesizing machine and

Received Sept. 27, 1994; revision accepted Jan. 26, 1995.

For correspondence or reprints contact: Irene Virgolini, MD, Department of Nuclear Medicine, University of Vienna, Währinger Gürtel 18-20, Ebene 3L, A-1090 Vienna, Austria.

TABLE 1
Patients' Diagnoses and Iodine-123-VIP Receptor Imaging Results

Patient no.	Sex	Age (yr)	Histological diagnosis	Size (diameter)	VIP receptor result
1	F	39	Pancreatic adenocarcinoma	Surgery, 2 cm	Positive
2	M	63	Pancreatic adenocarcinoma	CT, 4 cm	Positive
3	M	55	Liver metastases pancreatic adenocarcinoma*	CT, 1-4 cm	Positive
4	M	48	Liver metastases lymph node metastases colonic adenocarcinoma*	CT, 2-4 cm CT, 1-2 cm	Negative Positive
5	M	60	Liver metastases colonic adenocarcinoma*	CT, 2-3 cm	Positive
6	M	46	Colonic adenocarcinoma*		Negative (postsurgery control)
7	F	51	Pheochromocytoma	Surgery, 4 cm	Negative
8	M	30	Pheochromocytoma	Surgery, 3 cm	Positive
9	F	56	Suspected pheochromocytoma	CT Negative	Negative
10	F	36	Medullary thyroid cancer	Surgery, 2 cm	Negative
11	F	31	Cervical lymph node metastasis medullary thyroid cancer*	Surgery, 1 cm	Positive
12	F	39	Medullary thyroid carcinoma*		Negative (postsurgery control)
13	F	46	Ileocecal carcinoid	Surgery, 2 cm	Positive
14	M	45	Pancreatic carcinoid*		Negative (postsurgery control)
15	F	85	Carcinoid syndrome	CT negative	Negative
16	F	50	Carcinoid syndrome	CT negative	Negative
17	M	43	Gastrinoma	Surgery, 5 cm	Negative
18	F	86	Zollinger-Ellison syndrome	CT negative	Positive [†]

*In these patients, the primary tumor was resected at the time of VIP receptor scanning.

[†]In this patient, persistent elevation of serum gastrin as well as the presence of gastric and duodenal ulcerations strongly suggested the presence of a gastrinoma, but a primary tumor site could not be detected conventionally. VIP receptor scanning indicated a lesion in the small intestine, but surgery was not performed because of the patient's age.

labeled with ¹²³I using a modified lodogen method (19): 50 µg VIP in 10 µl 0.5 M phosphate buffer (pH 7.5), 10 µl 0.5 M phosphate buffer (pH 7.5) per 100 µl reaction volume, 17 ng KI carrier in 5 µl H₂O₂, the required activity of ¹²³I-Nal (specific activity >100 mCi/ml 0.01 M NaOH, about 0.005 nmole I/mCi; ¹²⁵I/¹²³I < 5 × 10⁻⁵; ¹²⁴I/¹²³I < 1 × 10⁻⁶) and 6 µg lodogen (per 100 µl reaction volume) in 5 µl phosphate-buffered saline (PBS) suspension (prepared freshly by dissolving 6 mg lodogen in 100 µl acetone and Vortex-mixing with 4900 µl PBS). The reaction mixture (about 200 µl, pH 7.5) was slowly stirred at room temperature for 30 min and injected quantitatively into a preparative HPLC system (column: RP C18, 5 µm, 4 × 250 mm; eluant: 74% (volume/volume) aqueous TEAF (triethylammonium-formiate, 0.25 M, pH 3, 26% (volume/volume) acetonitrile at 1 ml/min). After elution of the first ¹²³I-VIP peak, the eluant was changed to 60% aqueous TEAF and 40% acetonitrile. The column effluent passed through a scintillation radioactivity detector and UV (280 nm) detector in series. The system was calibrated with unlabeled VIP and enabled collection of pure radioiodinated VIP, separated from unlabeled VIP, reagents and inorganic iodide. The eluant was evaporated at reduced pressure, the product was dissolved in PBS containing 0.1% (weight/volume) Tween 80 (Koch-Light Lab. Ltd., Colnbrooke, UK) and 0.1% (weight/volume) human serum albumine (HSA). The final product was filtered through a sterile Millex GV 0.2 µm membrane (Millipore, Milford, MA).

Iodine-123-VIP was analyzed by analytical high-performance

liquid chromatography (HPLC) (corresponding to the preparative system, however, using a dedicated analytical column). Unlabeled VIP was determined by comparison with standards containing trace amounts of VIP. Radiochemical composition was assessed by the radioactive peak spectrum. Free radioiodide was determined by horizontal zone electrophoresis on Whatman 3 MM paper, 0.1 M barbital buffer, pH 8.6, using a field of 300 V for 10 min.

Biologic activity of the final radiolabeled product was determined in various in vitro tests, including studies on DNA-synthesis (³H-thymidine-incorporation) and ³²P-ATP-induced tyrosine kinase activity as described previously (11,19,20). These tests were performed using HT29 colonic adenocarcinoma cells and A431 mammary epidermoid carcinoma cells. For each series of experiments, about 5 × 10⁷ cells were used. Six independent experiments were performed with each cell line. Briefly, the effect of labeled or unlabeled VIP (concentration range 0.1 to 100 nmole/liter) on DNA synthesis was studied after addition of ³H-thymidine (specific activity 2.1 Ci/mmole, Amersham International, UK) to the cells following an incubation for 6 hr and measuring the trichloroacetic acid precipitable radioactivity in a liquid scintillation counter. In the phosphorylation assay, the cells were incubated with labeled or unlabeled VIP (concentration range 0.1 to 100 nmole/liter) for 30 min at 22°C. Phosphorylation was then initiated by addition of 100 mCi ³²P-ATP (specific activity: 111 GBq/mmole, Amersham International, Buckinghamshire, UK). After incubation for 10 min at 4°C in PBS/Triton buffer, cells were

washed twice and the extent of phosphorylation was quantified by measuring the remaining radioactivity in a liquid scintillation counter. The concentration causing half-maximal elevation (EC_{50}) was estimated from the dose-response curve.

Patients

The protocol for ^{123}I -VIP administration to patients was approved by the Ethical Committee of the Medical Faculty of the University of Vienna. All patients gave written informed consent. Whole-body biodistribution and dosimetry of ^{123}I -VIP were evaluated in 18 patients (Table 1) who had been referred for suspected VIP receptor-positive tumors (2,11). Patients reported in this study were not included in our previous article (2). To avoid significant variations in absorbed radiation dose estimation, patient selection was based on the following criteria:

1. Patients with unknown tumor masses after surgery.
2. Patients with small-sized intestinal or medullary thyroid tumors (1–2 cm in diameter).
3. Patients with negative VIP scan results.

The study protocol included whole-body gamma camera imaging as well as blood, urine and feces collections over 24 hr (see below). In all patients, diagnoses and stage of the disease were established according to WHO criteria. The location and size of primary tumors and/or spread of metastases were investigated by conventional CT, radiography, colonoscopy or by surgery.

Iodine-123-VIP was administered as a single intravenous bolus injection in 3 ml 0.9% NaCl solution (172 ± 17 MBq (4.65 ± 0.5

mCi); <300 pmole ($<1 \mu\text{g}$) VIP/patient). To record potential side effects of VIP, blood pressure and heart rate were monitored during peptide application. The patients received 400 mg sodium perchlorate three times daily over 3 days and 65 mg potassium iodide twice daily over 2 days for thyroid blockage.

Gamma Camera Imaging

Standard techniques were applied for recording and visualization. Planar and SPECT acquisitions were performed with a large field of view gamma camera equipped with a low-energy, general-purpose collimator. At the time of ^{123}I -VIP administration, the field of view covered the abdomen and some of the thorax, except in three patients (Table 1) with medullary thyroid gland cancer in whom the field of view covered the head and some of the thorax. Sequential images were recorded every minute for 30 min (matrix 128×128 pixels). Whole-body acquisition was performed simultaneously in anterior and posterior views using a double-headed gamma camera (matrix 256×1024 pixels, 20 cm/min). Anterior and posterior images were obtained using a parallel-hole collimation and a 20% symmetric energy window with a photopeak of 159 keV. Serial whole-body images were obtained 0.5–1, 2–4, 6–8 and 18–26 hr postinjection. If indicated, planar left and right lateral acquisitions also were performed, usually after the first whole-body scan within less than 1 hr after injection (matrix 128×128 pixels, 300 kcts preset).

Blood, Urine and Feces Collection

Blood samples were collected directly before injection and after 1, 3, 5, 8, 15, 20, 30, 60, 120 min and 4, 8, 16 and 24 hr. Urine was obtained after injection of VIP for the following intervals: 0–4, 4–8, 8–16 and 16–24 hr. In four patients, feces was collected over a 24-hr period.

Radioactivity in blood, urine or feces was counted in an automatic well gamma counter and expressed as Becquerels per milliliter. The counting efficiency of the system was determined by counting a calibrated source of ^{123}I with similar geometry to that of the samples. Radioactivity measurements were corrected for physical decay of ^{123}I . Radioactivity in the urine or feces was multiplied by the urine/feces volume to express radioactivity in the

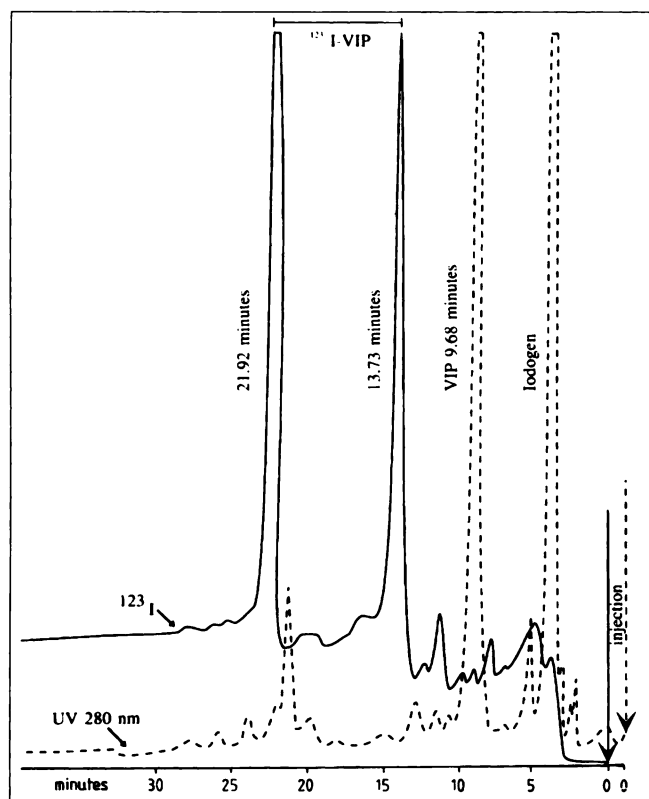


FIGURE 1. Preparative HPLC of ^{123}I -VIP. After injection of ^{123}I -VIP into the HPLC system, the radioactivity detector signal (full line) and the UV (280 nm) detector signal (dashed line offset to the right) were recorded. Iodine-123-VIP (2 peaks, labeled on both tyrosine residues in position 10 and 22) collected from the HPLC system was fully separated from unlabeled VIP.

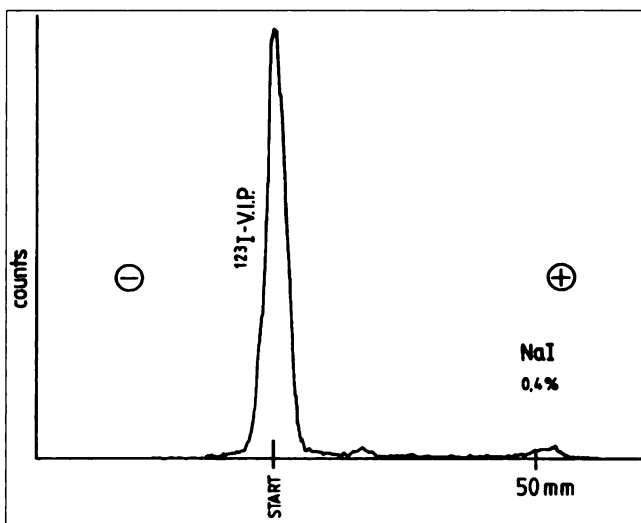


FIGURE 2. Horizontal zone electrophoresis of ^{123}I -VIP. Iodine-123-VIP remained at the application point, whereas I⁻ migrated to the indicated zone. Radiochemical purity was $>97\%$ 2 hr after labeling and remained stable for at least 24 hr.

TABLE 2
Tritiated Thymidine Uptake and Phosphorus-32-ATP-Induced Tyrosine Kinase Activity in Response to Unlabeled and Iodinated VIP

	³ H-thymidine uptake		³² P-ATP-Incorporation	
	Unlabeled VIP	¹²³ I-VIP	Unlabeled VIP	¹²³ I-VIP
A431 cells	4.8 ± 1.9	5.1 ± 2.0	6.7 ± 2.8	6.5 ± 3.1
HT29 cells	6.2 ± 2.3	5.9 ± 2.4	8.6 ± 3.2	7.3 ± 3.1

Thymidine incorporation was determined as a marker for DNA synthesis, and ATP incorporation as a marker of tyrosine kinase activity according to results from our previous study (11). Both unlabeled and labeled VIP dose-dependently induced thymidine uptake and tyrosine kinase activity in A431 mammary epidermoid carcinoma cells as well as in HT29 colonic adenocarcinoma cells. The EC₅₀ values (concentrations causing half-maximal elevation) listed are of similar magnitude, indicating that unlabeled and labeled VIP displayed the same biological activity. The mean values of six independent experiments ± s.d. are listed. All values are in nanomoles per liter.

samples as the percent of the injected ¹²³I-VIP dose. Peptide-bound ¹²³I in blood was analyzed using 10% (final) trichloroacetic acid and measuring the precipitated activity in the gamma counting system.

Absorbed Dose Calculations

Regions of interest (ROIs) were drawn on every subject at each time point. The geometric mean of anterior and posterior counts was calculated for large ROIs of the lungs and urinary bladder. In addition, ROIs were drawn for liver, kidneys, gonads and thyroid gland using the software written for the Toshiba (Tokyo, Japan) computer. All gamma camera data were corrected for background counts. Time-activity curves were fitted to evaluate the fraction of activity at reference time and effective half-life of each source organ from the average relative ROI activities. These biodistribution data as well as urine kinetics and the measured radioactivity in the feces were used for organ dose calculation on the basis of the MIRD concept (21). Radionuclidic impurities in the ¹²³I preparation were negligible and were therefore not considered in the radiation dose calculations. Absorbed organ doses were calculated by applying tabulated specific absorbed fractions (22) and the LUPED Version 1.0 computer program (23). The effective dose, as defined by the International Commission on Radiological Protection, also was calculated (24).

RESULTS

Radiochemical Purity and Bioactivity of Iodine-123-VIP

Using preparative HPLC, the ¹²³I-VIP product was obtained in an average radiochemical yield of 72% (range 55%–80%). Both tyrosine residues of the VIP molecule (in positions 10 and 22) were labeled with ¹²³I as indicated in Figure 1. Iodine-123-VIP collected from the HPLC system was fully separated from unlabeled VIP as well as from reagents and inorganic iodine species. The radiochemical purity was more than 97% 2 hr after labeling; the percentage of unbound iodide did not change over 24 hr (Fig. 2). The biologic activity of unlabeled and labeled VIP were almost identical as assessed by experiments on DNA synthesis (³H-thymidine uptake) and ³²P-ATP-induced tyrosine kinase activity (Table 2). Moreover, the binding activity of unlabeled and labeled VIP were identical as determined in radioreceptor assays using various specific activities of ¹²³I-VIP (11).

Safety

After intravenous injection of ¹²³I-VIP, no side effects were noted with the exception of transient decreases of both systolic and diastolic blood pressures during the initial minutes after peptide application. Blood pressure 5 min after injection ¹²³I-VIP decreased by 5%–10% in the mean (systolic blood pressure: 146 ± 23 before versus 137 ± 19 mmHg after injection; diastolic blood pressure: 87 ± 13 before versus 78 ± 19 after injection) and reached baseline values within 10 min after injection.

Whole-Body Biodistribution of Iodine-123-VIP

After intravenous injection, ¹²³I-VIP was rapidly cleared from the circulation as measured by increasing lung-to-heart ratios (Fig. 3). Radioactivity in the blood rapidly decreased to less than 5% of the injected activity within the first 5 min after injection of ¹²³I-VIP (Fig. 4). Peptide-bound radioactivity in blood amounted to 89% ± 6% at 0.5 hr, to 65% ± 13% at 1 hr, 57% ± 14% at 2 and to 44% ±

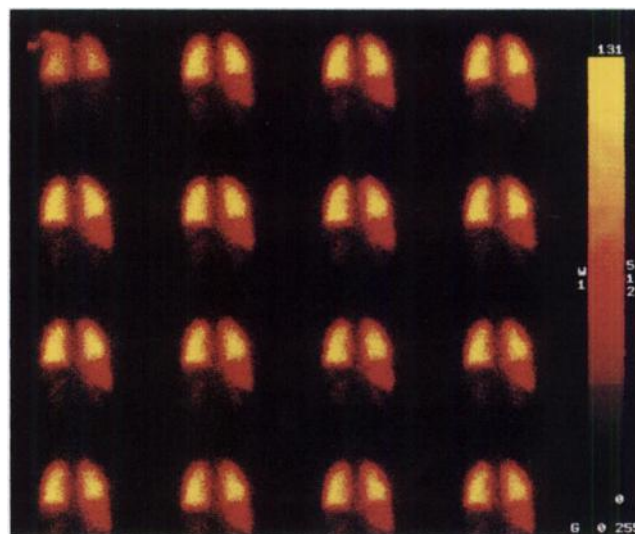


FIGURE 3. Iodine-123-VIP receptor scanning. After intravenous injection, ¹²³I-VIP (153 MBq (4.1 mCi)/300 pmole) rapidly bound to the lungs. Sequential posterior images were acquired during the first 8 min after ¹²³I-VIP application (1 frame/30 sec).

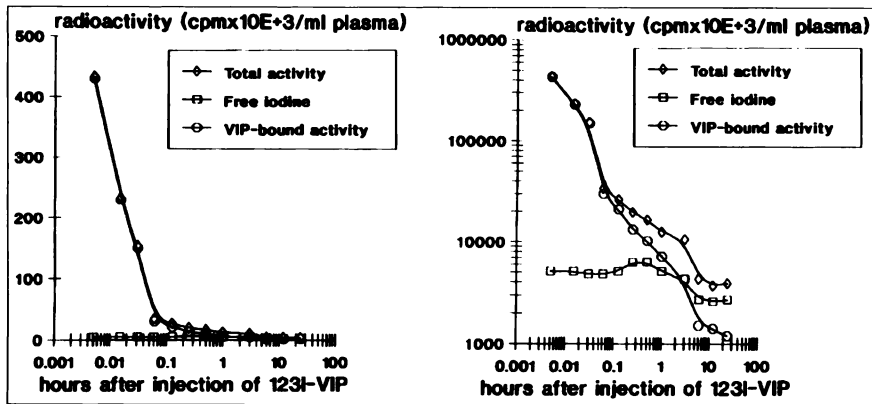


FIGURE 4. Blood kinetics of ^{123}I -VIP. After intravenous injection, ^{123}I -VIP was rapidly cleared from the circulation with a calculated half-life of 0.75 ± 0.15 min (left). Up to 2 hr postinjection, the remaining radioactivity in the plasma was mainly peptide-associated (right). Plasma activity (<5% of wholebody activity at all time points) slowly decreased with time and the fraction of free iodine increased over 24 hr. A typical blood kinetic curve derived from Patient 6 (Table 1) is depicted.

319% 4 hr after injection of ^{123}I -VIP (in terms of remaining plasma activity at these time points).

The accumulation of ^{123}I -VIP in the lungs reached its maximum within the first 10 min of imaging presenting the lung as the primary site of ^{123}I -VIP uptake. On average, radioactivity measured over the lungs represented $40.3\% \pm 6.6\%$ of the whole-body uptake at 0.7 ± 0.2 hr after injection and decreased to 21.5 ± 7.0 at 3.5 ± 0.5 hr, to $13.9\% \pm 3.2\%$ at 7.2 ± 1.4 hr and to $8.2\% \pm 4.0\%$ at 22.5 ± 2.3 hr (Table 3). Iodine-123-VIP uptake by the liver amounted to $6.5\% \pm 1.2\%$ and by the kidneys to $4.2\% \pm 2.4\%$ of the injected radioactivity at 0.7 ± 0.2 hr after injection. Cumulative radioactivity excreted into the urine amounted to $37\% \pm 16\%$ of the injected activity at 4, $68\% \pm 12\%$ at 8, $82\% \pm 16\%$ at 16, and $90\% \pm 6\%$ at 24 hr after injection of ^{123}I -VIP (Fig. 5). Cumulative radioactivity in the feces was $5\% \pm 1\%$ percent ($n = 4$) of the injected activity after 24 hr. Calculated uptakes for spleen and gonads were less than 0.5% of the total injected activity at all time points.

Radiation Absorbed Doses

The lungs and urinary bladder were the primary source organs. The radioactivity over the normal liver and kidneys was only hardly distinguishable from the surrounding intestinal tissue. Individual ROIs were fitted over these organs (liver, kidneys) as well as over the gonads and thyroid gland. Radioactivity at sites of small-sized intestinal tumors/metastases was negligible in the dosimetry calculations. The

effective half-lives and radiation absorbed organ doses are presented in Tables 4 and 5. The highest radiation absorbed doses were calculated for the lungs [$67 \mu\text{Gy}/\text{MBq}$ ($248 \text{ mrad}/\text{mCi}$)], urinary bladder [$77 \mu\text{Gy}/\text{MBq}$ ($284 \text{ mrad}/\text{mCi}$)] and thyroid gland [$104 \mu\text{Gy}/\text{MBq}$ ($386 \text{ mrad}/\text{mCi}$)]. The absorbed dose to the gonads was less than $10 \mu\text{Gy}/\text{MBq}$ ($35 \text{ mrad}/\text{mCi}$). The effective dose was estimated to be $28 \mu\text{Sv}/\text{MBq}$ ($104 \text{ mrem}/\text{mCi}$).

Iodine-123-VIP Imaging

As listed in Table 1, serial whole-body scanning for dosimetry calculations was performed in three patients with pancreatic adenocarcinoma, in three patients with colonic adenocarcinoma, in two patients with pheochromocytoma, in one patient with suspected pheochromocytoma, in three patients with medullary thyroid gland cancer, in two patients with carcinoid tumors, in two patients with carcinoid syndrome, in one patient with gastrinoma and in one patient with Zollinger-Ellison syndrome. Diagnoses and disease stage were established by CT or surgery. In two patients (Patients 9, 18), an endocrine tumor was suspected but could not be verified by conventional modalities.

VIP receptor scanning visualized pancreatic adenocarcinomas in two patients (Patients 1, 2; Fig. 6). A primary CT-negative ileocecal carcinoid tumor was detected by VIP receptor scanning in Patient 13 and could be verified surgically. Lymph node metastases were seen in two patients (Patients 4, 11) and liver metastases in two of three pa-

TABLE 3
Tissue Biodistribution as a Function of Time after Intravenous Injection of Iodine-123-VIP

Organ	Time postinjection of ^{123}I -VIP (hr)			
	0.7 ± 0.2 (0.5–1)	3.5 ± 0.5 (2–4)	7.2 ± 1.4 (6–8)	22.5 ± 2.3 (18–26)
Lung	40.3 ± 6.6 (26–52)	21.5 ± 7.0 (13–34)	13.9 ± 3.2 (10–24)	8.2 ± 4.0 (6–14)
Liver	6.5 ± 1.2 (4–8)	3.5 ± 1.5 (2–6)	2.3 ± 1.3 (1–4)	1.5 ± 1.2 (0.5–3)
Kidneys	4.2 ± 2.4 (2–7)	3.2 ± 1.9 (2–6)	2.2 ± 0.9 (1.5–4)	1.1 ± 0.4 (0.5–2)
Bladder	4.5 ± 2.5 (2–8)	7.4 ± 4.8 (2–9)	6.4 ± 2.7 (2.5–9)	4.3 ± 2.9 (2.5–7.5)
Thyroid	0.5 ± 0.2 (0.1–0.9)	0.4 ± 0.2 (0.1–0.8)	0.7 ± 0.2 (0.9 \pm 0.3)	0.8 ± 0.3 (0.4–1.2)

Values listed are means \pm s.d (numbers in parentheses are range values). All values are expressed as the percent whole-body activity at various time points after injection of ^{123}I -VIP.

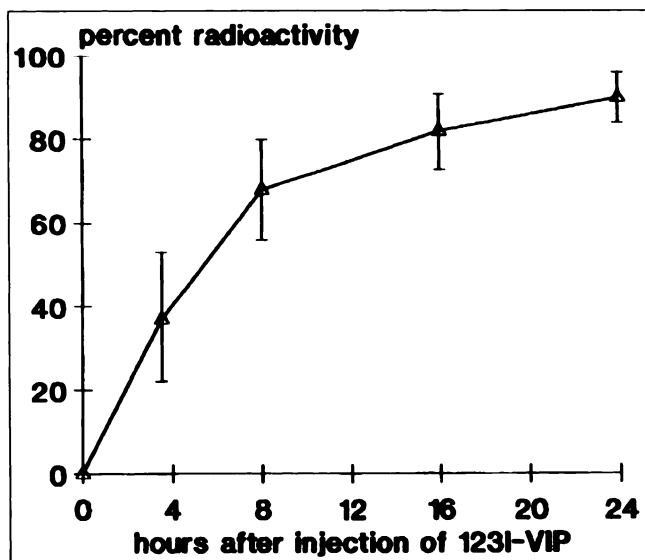


FIGURE 5. Radioactivity was excreted through the urinary tract and cumulative radioactivity measured in the urine is shown.

tients. In Patient 18, who had Zollinger-Ellison syndrome, an accumulation of ^{123}I -VIP was visualized in the small intestine, most probably due to the primary site of the gastrinoma. Negative VIP scans were obtained in three patients (Patients 6, 12, 14) after removal of the primary tumors, in one patient with verified pheochromocytoma (Patient 7), in one patient with suspected pheochromocytoma, in one patient with medullary thyroid cancer (Patient 10), in one patient with gastrinoma (Patient 17) and in two patients with carcinoid syndrome in whom no tumor could be detected by conventional techniques. A summary of VIP scanning data is provided in Table 1.

DISCUSSION

Recent studies have shown that various gastrointestinal tumors express substantial amounts of VIP receptors. Based on these observations, we have developed a receptor

TABLE 5
Estimation of the Effective Dose (E) for Iodine-123-VIP

Organ/Tissue (g)	Organ dose H_T		
	($\mu\text{Gy}/\text{MBq}$)	(mrad/mCi)	% (E)
Gonads	9.4	34.8	6.7
Red bone marrow	11.7	43.3	5.0
Colon	19.8	73.26	8.5
Lungs	67.0	247.9	28.8
Stomach	12.3	45.5	5.3
Urinary bladder	76.7	283.8	13.7
Breast	10.2	37.7	1.8
Liver	25.0	92.5	4.5
Esophagus	28.5	105.5	5.1
Thyroid	104.3	385.9	18.7
Skin	6.1	22.6	0.2
Bone surface	16.0	59.2	0.6
Kidneys	52.9	195.7	—
Remainder of body	13.2	48.8	1.1
Effective dose	28 $\mu\text{Sv}/\text{MBq}$ (104 mrem/mCi)		

Dose estimates were performed on the basis of gamma camera measurements, urinary and fecal excretion. Organs for which a tissue weighting factor is specified contribute to the effective dose. The other equivalent organ doses are considered in the calculation of the remainder of the body (tissue-mass weighted mean).

scintigraphic technique by using ^{123}I -VIP as radioligand (2).

VIP is a well-characterized vasoactive polypeptide causing systemic vasodilation and hypotension in the picomolar range (2,3). In the present study, radiolabeled VIP was purified by preparative HPLC to obtain a high-specific activity of $>500 \text{ TBq}/\text{mmole}$. Use of this high-specific activity preparation of ^{123}I -VIP allowed intravenous bolus injection of ^{123}I -VIP to humans without severe side effects, although a transient drop in blood pressure values was observed during the initial minutes after peptide application. Furthermore, the biologic activities of unlabeled and ^{123}I -labeled VIP, as assessed by thymidine-uptake and

TABLE 4
Whole-body Biodistribution of Iodine-123-VIP*

Source organ	Time after injection of ^{123}I -VIP (hr)				fraction F (t = 0)	T_{eff} (hr)	T_{biol} (hr)
	t = 0.5 hr = 100%	t = 3.5 hr = 76.3%	t = 7.2 hr = 38.8%	t = 22.5 hr = 13.0%			
Gonads	0.008	0.0025	0.00011	<0.000013	0.020	1.0	1.1
Lungs	0.403	0.164	0.054	0.0107	0.494	2.2	3.0
Urinary bladder	0.045	0.0565	0.0248	0.0056	0.045†	6.3	11.2
Liver	0.065	0.027	0.0089	0.002	0.080	2.7	3.4
Thyroid	0.005	0.003	0.0027	0.00104	0.016	10.5	52.0
Kidneys	0.042	0.027	0.0085	0.0014	0.098	2.8	3.6
Intestinal	0.009	0.008	0.0027	0.0015	0.092	9.4	32.7
Remainder of body	0.443	0.352	0.187	0.056	0.514	5.1	8.3

*Correction of data from Table 3 for t = 0.5 hr, fractions of activity at t = 0 and effective (T_{eff}) and biological half-lives (T_{biol}) of ^{123}I -VIP.

†Estimation of cumulated activity starting with t = 3.5 hr.

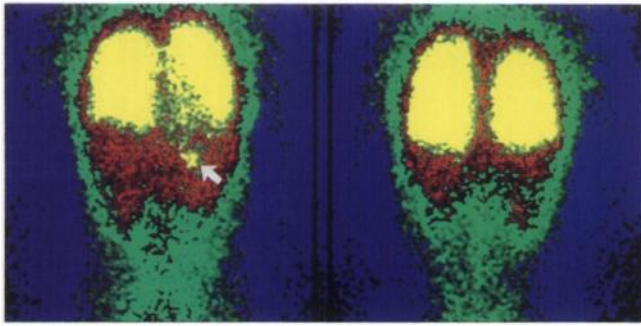


FIGURE 6. VIP receptor scanning of a primary adenocarcinoma was performed after injection of 150 MBq (4 mCi) ^{123}I -VIP (300 pmole). A small focus of ^{123}I -VIP was visualized in the pancreatic area (arrow) during 2-hr whole-body scanning. The tumor-to-intestinal background ratio was 2.9 (right, anterior image; left, posterior image). CT scanning performed on the same day confirmed significant regression of the primary tumor mass and disappearance of lymph node metastases.

ATP-induced tyrosine kinase activity experiments, were identical.

So far, little is known about the biodistribution and in vivo binding of VIP. In this study, biodistribution of ^{123}I -VIP revealed a unique pattern with high uptake by the lungs, confirming results in a recent report in experimental animals (25). Radiolabeled VIP was rapidly cleared from the circulation with a calculated half-life of approximately 1 min. No substantial uptake by liver, spleen or normal gastrointestinal tissue (compared to lung activity) was noted. For the detection of gastrointestinal tumors, the unique biodistribution of ^{123}I -VIP is an apparent advantage over other iodinated peptides that are mainly excreted through the hepatobiliary system (1).

After injection of ^{123}I -VIP, the radioactivity was excreted into the urine with an effective half-life of 6.3 hr in the urinary bladder. We used 170 MBq (4.6 mCi) for each investigation, resulting in an effective dose of 4.76 mSv (476 mrem) that is comparable with the radioactive burden caused by other peptide tracers (26).

The unique biodistribution of ^{123}I -VIP and its favorable dosimetry was a prerequisite for the use of ^{123}I -VIP as a tumor-seeking tracer. So far, ^{123}I -VIP has successfully been used for the detection of gastrointestinal adenocarcinomas and endocrine tumors expressing receptors for ^{123}I -VIP (2). In this study, patients with small-sized or VIP receptor-negative tumors were selected for dose calculations. No substantial differences between patients with detectable (VIP receptor scan-positive) tumors versus VIP scan-negative patients were observed in VIP biodistribution behavior.

The molecular basis of interaction of VIP with organs, tissues or tumor cells is not completely understood. A number of recent observations suggest that VIP binds to its target cells by cell surface membrane receptors. These receptors have been detected in various organs and tissues, including the lung (17), intestinal epithelium (15,16) and on various tumor cells (11). In light of specific biodistribu-

tion of VIP and its high affinity for tumor cells, it is tempting to speculate that positive in vivo images obtained after injection of ^{123}I -VIP are due to VIP-VIP-receptor interactions.

CONCLUSION

Iodine-123-VIP is a promising peptide tracer with a favorable dosimetry, unique biodistribution and high affinity to normal lung tissue and various tumor cells.

ACKNOWLEDGMENTS

This study was supported in part by the Foundation of the Mayor of the City of Vienna, the Hochschuljubiläumsfonds, the Austrian National Bank and the Fonds zur Förderung der wissenschaftlichen Forschung in Österreich.

REFERENCES

- Lamberts SWJ, Bakker WH, Reubi JC, Krenning EP. Somatostatin receptor imaging in the localization of endocrine tumors. *N Engl J Med* 1990;323:1246-1249.
- Virgolini I, Raderer M, Kurtaran A, et al. Iodine-123-vasoactive intestinal peptide for the localization diagnosis of intestinal adenocarcinomas and endocrine tumors. *N Engl J Med* 1994;331:1116-1121.
- Said SI, Mutt V. Polypeptide with broad biological activity. Isolation from small intestine. *Science* 1970;169:1217-1218.
- Domschke S, Domschke W, Rösch W, et al. Vasoactive intestinal peptide: a secretin-like partial agonist for pancreatic secretion in man. *Gastroenterology* 1977;73:478-480.
- Bloom SR, Polak JM, Pearse AGE. Vasoactive intestinal peptide and watery diarrhea syndrome. *Lancet* 1973;2:14-16.
- Schwartz CJ, Kimberg DV, Sheerin HE, Field M, Said SI. Vasoactive intestinal peptide stimulation of adenylate cyclase and active electrolyte secretion in intestinal mucosa. *J Clin Invest* 1974;54:536-544.
- Said SI, Faloona GR. Elevated plasma and tissue levels of vasoactive intestinal polypeptide in the watery-diarrhea syndrome due to pancreatic, bronchogenic and other tumors. *N Engl J Med* 1975;293:155-160.
- Verner JV, Morrison AB. Islet cell tumor and a syndrome of refractory watery diarrhea and hypokalemia. *Am J Med* 1958;25:374-380.
- O'Dorisio MS, Wood CL, O'Dorisio TM. Vasoactive intestinal polypeptide as a neuromodulator of lymphocyte function: a review. *J Immunol* 1985;135:7925-7931.
- Ottaway CA. In vitro alteration of receptors for vasoactive intestinal peptide changes in the in vivo localization of mouse T cells. *J Exp Med* 1984;160:1054-1057.
- Virgolini I, Yang Q, Li SR, et al. Cross-competition between vasoactive intestinal peptide (VIP) and somatostatin for binding to tumor cell receptors. *Cancer Res* 1994;54:690-700.
- Pincus DW, DiCicco-Bloom EM, Black IB. Vasoactive intestinal polypeptide regulates mitosis, differentiation and survival of cultured sympathetic neuroblasts. *Nature* 1990;343:564-567.
- Haegerstrand A, Jonzon B, Dalsgaard CJ, Nilsson J. Vasoactive intestinal polypeptide stimulates cell proliferation and adenylate cyclase activity of cultured human keratinocytes. *Proc Natl Acad Sci USA* 1989;86:5993-5996.
- Cohn J. Vasoactive intestinal peptide stimulates protein phosphorylation in a colonic epithelial cell line. *Am J Physiol* 1987;16:G420-G424.
- Blum AM, Mathew R, Cook GA, et al. Murine mucosal T cells have VIP receptors functionally distinct from those on intestinal epithelial cells. *J Neuroimmunol* 1992;39:101-108.
- Prieto JC, Laburthe M, Rosselin G. Interaction with isolated intestinal epithelial cells from rat. *J Biochem* 1979;96:229-234.
- Paul S, Said SI. Characterization of receptors for vasoactive intestinal peptide solubilized from the lung. *J Biol Chem* 1987;262:158-162.
- Sreedharan SP, Patel DR, Huang JX, Goetzl EJ. Cloning and functional expression of a human neuroendocrine vasoactive intestinal peptide receptor. *Biochem Biophys Res Commun* 1993;193:546-553.
- Virgolini I, Angelberger P, Li SR, et al. Indium-111-labeled low density lipoprotein (LDL) binds with higher affinity to the human liver as compared to ^{123}I -labeled LDL. *J Nucl Med* 1991;32:2132-2138.
- Virgolini I, Sillaber C, Majdic O, et al. Characterization of prostaglandin

- binding sites expressed on human blood basophils. Evidence for a prostaglandin E₁, I₂ and D₂ receptor. *J Biol Chem* 1992;267:12700–12708.
21. Loevinger R, Budinger T, Watson E. *MIRD primer for absorbed dose calculations*. New York: Society of Nuclear Medicine; 1988.
 22. Cristy M, Eckerman KF. Specific absorbed fractions of energy at various ages from internal photon sources. Oak Ridge National Laboratory, ORNL/TM-8381, Oak Ridge, TN, 1987.
 23. Jarvis NS, Birchall A, James AC, Bailey MR, Dorrian MD. LUPED 1.0, personal computer program for calculating internal doses using the ICRP respiratory tract model. National Radiological Protection Board, Oxon, U.K., 1993.
 24. ICRP 1990 Recommendations of the International Commission on Radiological Protection. *ICRP publication 60*. Pergamon Press; Oxford: 1991.
 25. Hassan M, Refai E, Andersson M, Schnell PO, Jacobson H. In vivo dynamic distribution of ¹³¹I-VIP in the rat studied by gamma camera. *Nucl Med Biol* 1994;21:865–872.
 26. Johansson L, Mattson S, Nosslin B, Svegborn SR. Effective dose from radiopharmaceuticals. *Eur J Nucl Med* 1993;19:933–938.

FIRST IMPRESSIONS

Duplicated collecting system in an elongated left kidney?

For acquisition information, turn to page 1817.

